

Supporting Information for:

**Study of *para*-Quinone Methide Precursors Towards the Realkylation of Aged
Acetylcholinesterase**

Ryan J. Yoder[#], Qinggeng Zhuang, Jeremy M. Beck, Andrew Franjesevic, Travis G. Blanton[#],
Sydney Sillart, Tyler Secor, Leah Guerra, Jason D. Brown, Carolyn Reid, Craig A. McElroy[†],
Özlem Dogan Ekici[‡], Christopher S. Callam, Christopher M. Hadad^{*}

Department of Chemistry and Biochemistry, The Ohio State University, 100 West 18th Avenue,
Columbus, OH 43210, USA

[#]Department of Chemistry and Biochemistry, The Ohio State University, Marion Campus, 1465
Mt. Vernon Avenue, Marion, OH 43302, USA

[†]College of Pharmacy, The Ohio State University, 500 West 12th Avenue, Columbus, OH
43210, USA

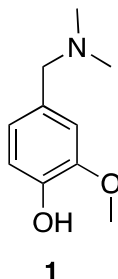
[‡]Department of Chemistry and Biochemistry, The Ohio State University, Newark Campus, 1179
University Drive, Newark, OH 43055, USA

Experimental

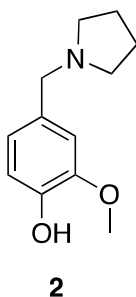
General. Solvents were distilled from the appropriate drying agents before use. Unless stated otherwise, all reactions were carried out under a positive pressure of nitrogen. Reactions were monitored by GC-MS (Agilent 6850, 5975C detector, Agilent HP-5MS, 30 m x 0.25 mm, 0.25 mm film column) and thin-layer chromatography (TLC) on silica gel 60 F₂₅₄ (0.25 mm, E. Merck). Spots were detected under UV light, phosphomolybdic acid (PMA) in ethanol, or *p*-anisaldehyde. Solvents were evaporated under reduced pressure and below 40 °C (bath). Organic solutions of crude products were dried over anhydrous MgSO₄. Chromatography was performed on silica gel 60 (40-60 μM). The ratio between silica gel and crude product ranged from 100 to 50:1 (w/w). Melting points are uncorrected. ¹H NMR spectra were recorded at 400 MHz, and chemical shifts are referenced to CDCl₃ (7.24). ¹³C NMR spectra were recorded at 100 MHz, and ¹³C shifts are referenced to CDCl₃ (77.23, CDCl₃). Electrospray mass spectra were recorded on samples suspended in mixtures of water and methanol.

General Procedures for Reductive Amination.

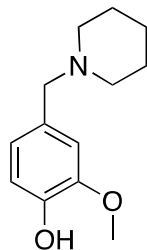
The amine (dimethyl amine, pyrrolidine, piperidine, or morpholine, 23mmol, 3 eq.) was stirred with methanol (20 mL) while concentrated HCl (0.7 mL) was added dropwise over 2-3 min. After acid was added, the reaction was covered until HCl fumes cleared. Vanillin (1.2 g, 7.9 mmol, 1 eq.) was then added to the reaction and allowed to stir until the solution was homogeneous. Sodium cyanoborohydride (1.1 eq.) was added in one portion and the solution was stirred for at least 1 h (25 °C). The solution was heated to reflux for 2 h. After cooling to room temperature (rt, 25 °C), distilled water (30 mL) was added and allowed to stir for 5 min. The solution was extracted with dichloromethane (3 x 40 mL) and the organic layers were combined and dried. The organic solution was evaporated under reduced pressure to yield a crude oil. The crude product was purified by chromatography (15:1, petroleum ether/EtOAc) to obtain **1-4** as a colorless oils and with the following yields: (**1**, 78 %), (**2**, 83%), (**3**, 80%), and (**4**, 85%). Compounds (**1-4** and **1-HCl - 4-HCl**) were characterized by ¹H NMR analysis, ¹³C NMR, FT-IR and ESI mass spectrometry. The purity of sample (**1-4** and **1-HCl - 4-HCl**) were determined by ¹H NMR analysis.



Synthesis of 4-((dimethylamino)methyl)-2-methoxyphenol (**1**): ^1H NMR (400 MHz, CDCl_3 , δH) 6.85-6.68 (m, 3H), 3.73 (s, 3H), 3.34 (2H), 2.21 (s, 6H); ^{13}C NMR (100 MHz, CDCl_3 , δC) 147.2, 145.5, 130.0, 122.3, 114.4, 112.0, 64.3 55.8, 45.2; IR (KBr disc) 3085, 2940, 1636, 1615, 1524 cm^{-1} . ESI (m/z) $\text{C}_{10}\text{H}_{16}\text{NO}_2^+$: calc. 182.1176; obs. 182.1168.

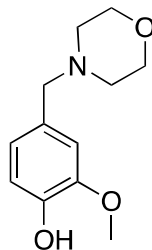


Synthesis of 2-methoxy-4-(pyrrolidin-1-ylmethyl)phenol (**2**): ^1H NMR (400 MHz, CDCl_3 , δH) 6.86-6.74 (m, 3H), 3.79 (s, 3H), 3.53 (s, 2H), 2.52-2.49 (m, 4H), 1.79-1.75 (m, 4H); ^{13}C NMR (100 MHz, CDCl_3 , δC) 146.9, 145.1, 131.0, 122.0, 114.3, 111.9, 60.8, 56.0, 54.2, 23.6; IR (KBr disc) 3080, 2942, 2873, 1633, 1615 cm^{-1} . ESI (m/z) $\text{C}_{12}\text{H}_{18}\text{NO}_2^+$: calc. 208.1332; obs. 208.1330.



3

Synthesis of 2-methoxy-4-(piperidin-1-ylmethyl)phenol (**3**): ^1H NMR (400 MHz, CDCl_3 , δH) 6.89-6.72 (m, 3H), 3.89 (s, 3H), 3.41 (s, 2H) 2.37-2.34 (m, 4H), 1.58 (p, 4 H, 5.6 Hz), 1.43-1.41 (m, 2H); ^{13}C NMR (100 MHz, CDCl_3 , δC) 146.7, 145.0, 129.2, 122.5, 114.3, 112.1 63.8, 56.2, 54.5, 25.9, 24.5; IR (KBr disc) 2940, , 1636, 1615, 1524 cm^{-1} . ESI (m/z) $\text{C}_{13}\text{H}_{20}\text{NO}_2^+$: calc. 222.1489; obs. 222.1483.

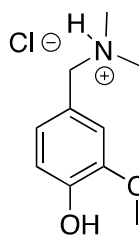


4

Synthesis of 2-methoxy-4-(morpholinomethyl)phenol (**4**): ^1H NMR (400 MHz, CDCl_3 , δH) 6.85-6.73 (m, 3H), 3.87 (s, 3H), 3.70-3.67 (m, 4H), 3.40 (s, 2H), 2.42-2.40 (m, 4H); ^{13}C NMR (100 MHz, CDCl_3 , δC) 146.7, 145.1, 129.5, 122.4, 114.2, 111.9, 67.1, 63.5, 56.1, 53.7. IR (KBr disc) 2942, 1635, 1610, 1520 cm^{-1} . ESI (m/z) $\text{C}_{12}\text{H}_{18}\text{NO}_3^+$: calc. 224.1281; obs. 224.1278.

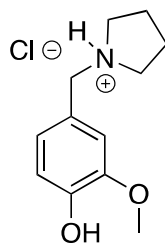
HCl Salt Formation General Method.

The neutral crude product was dissolved in methanol (15 mL) and heated slightly to aid in complete dissolution. 5 M HCl (1.52 mL) was added to the mixture to a pH of 2-3. The solvent was removed under reduced pressure. The crude product was triturated with acetone (3 x 3 mL) and isolated to yield the corresponding HCl salt: **1-HCl** (65 %), **2-HCl** (71 %), **3-HCl** (76 %), **4-HCl** (81%). The purity of sample (1-4 and 1-HCl - 4-HCl) were determined by ¹H NMR analysis.



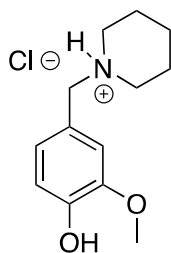
1-HCl

Synthesis of 1-(4-hydroxy-3-methoxyphenyl)-*N,N*-dimethylanaminium chloride (**1-HCl**): ¹H NMR (400 MHz, CD₃OD, δH) 7.05 (s, 1H), 6.95 (s, 2H), 4.20 (s, 2H), 3.87 (s, 3H), 2.83 (s, 6H); ¹³C NMR (100 MHz, CD₃OD, δC) 150.11, 148.86, 126.8, 124.1, 118.2, 117.0, 63.5, 58.4, 44.3; IR (KBr discs) 3544, 3411, 3237, 2709, 1638, 1616 cm⁻¹. ESI (m/z) C₁₀H₁₆NO₂⁺: calc. 182.1176; obs. 182.1161.



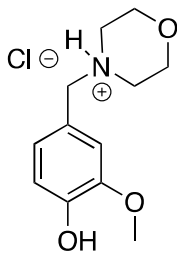
2-HCl

Synthesis of 1-(4-hydroxy-3-methoxybenzyl)pyrrolidin-1-ium chloride (**2-HCl**): ^1H NMR (400 MHz, CD_3OD , δH) 7.11 (s, 1H), 6.99-6.97 (m, 2H), 4.28 (s, 2H), 3.92 (s, 3H), 3.51-3.46 (m, 2H), 3.20-3.15 (m, 2H), 2.19-2.01 (m, 2H), 2.03-1.95 (m, 2H); ^{13}C NMR (100 MHz, CD_3OD , δC) 150.2, 148.6, 126.2, 125.4, 118.3, 116.6, 60.4, 58.5, 55.9, 24.9; IR (KBr discs) 3550, 34780, 3387, 1640 cm^{-1} . ESI (m/z) $\text{C}_{12}\text{H}_{18}\text{NO}_2^+$: calc. 208.1332; obs. 208.1325.



3-HCl

Synthesis of 1-(4-hydroxy-3-methoxybenzyl)piperdin-1-ium chloride (**3-HCl**): ^1H NMR (400 MHz, CD_3OD , δH) 7.17-6.98 (m, 3H), 4.30 (s, 2H), 3.92 (s, 3H), 3.51-3.47 (m, 2 H), 3.03-2.98 (m, 2H), 1.96-1.81 (m, 2H), 1.79-1.46 (m, 4 H); ^{13}C NMR (100 MHz, CD_3OD , δC) 147.7, 145.1, 124.3, 120.4, 116.0, 113.9, 56.3, 55.2, 52.9, 22.5, 21.1; IR (KBr discs) 3550, 3479, 3412, 3236, 2956, 1638, 1617 cm^{-1} . ESI (m/z) $\text{C}_{13}\text{H}_{20}\text{NO}_2^+$: calc. 222.1489; obs. 222.1495.



4-HCl

Synthesis of 4-(4-hydroxy-3-methoxybenzyl)morpholin-4-ium chloride (**4-HCl**): ^1H NMR (400 MHz, CD_3OD , δH) 7.11 (s, 1H), 6.99-6.96 (m, 2H), 4.28 (s, 2 H), 4.28-3.92 (m, 7H), 3.38-3.32 (m, 3H), 3.68-3.65 (m, 4H); ^{13}C NMR (100 MHz, CD_3OD , δC) 150.1, 149.0, 127.3, 122.7,

118.2, 117.5, 66.2, 63.3, 58.5, 53.6; IR (KBr discs) 3550, 3430, 1638, 1617 cm^{-1} . ESI (m/z) $\text{C}_{12}\text{H}_{18}\text{NO}_3^+$: calc. 224.1281; obs. 224.1277.

See the NMR spectra in a file (appendix NMRDataSet.pdf).

Alkylation of model nucleophiles

(1.2 eq) of nucleophile (benzyl alcohol, piperidine, pyrrolidine, p-methylbenzenethiol) was added to QMPs (**1-4**) or (**1-HCl** – **4-HCl**) (100 mg, 1. eq.) in 50:50 $\text{H}_2\text{O}:\text{CH}_3\text{OH}$ (~5 mL). The reaction was allowed to heat for 3 h at 100 °C. The reaction was allowed to cool to rt and was then extracted with diethyl ether (3 × 3 mL). The organic layers were collected and dried. The dried organic layers were concentrated under reduced pressure to yield the crude product. The compounds in the crude product were separated by column chromatography (15:1, petroleum ether/EtOAc). Solvents in the eluates were evaporated to obtain the pure product, which was weighed to quantify the species. The resulting compounds were characterized by ^1H NMR, ^{13}C NMR and ESI mass spectrometry.

2-methoxy-4-((*p*-tolylthio)methyl)phenol). R_f 0.20 (15:1, petroleum ether/EtOAc). ^1H NMR (400 MHz, CDCl_3 , δH) 7.20 (d, 2H, $J = 7.5$ Hz), 7.07 (d, 2H, $J = 7.5$ Hz), 6.80-6.70 (m, 3H), 3.99 (s, 2H), 3.81 (s, 3H), 2.38 (s, 3H). ^{13}C NMR (100 MHz, CDCl_3 , δC) 148.6, 148.0, 136.6, 132.4, 130.9, 130.0, 129.3, 120.7, 111.8, 110.7, 55.8, 39.7, 20.9. ESI (m/z) $\text{C}_{15}\text{H}_{17}\text{O}_2\text{S}^+$: calc. 261.0949; obs. 261.0953

2-methoxy-4-(pyrrolidin-1-ylmethyl)phenol. The crude product was purified by chromatography (15:1, petroleum ether/EtOAc) to obtain the product as a clear oil. The ^1H NMR was compared to our previously prepared materials. ESI was also verified to match $\text{C}_{12}\text{H}_{18}\text{NO}_2^+$.

2-methoxy-4-(piperidin-1-ylmethyl)phenol. The crude product was purified by chromatography (15:1, petroleum ether/EtOAc) to obtain the product as a clear oil. The ^1H NMR was compared to our previously prepared materials. ESI was also verified to match $\text{C}_{13}\text{H}_{20}\text{NO}_2^+$.

4-((benzyloxy)methyl)-2-methoxyphenol. The crude product was purified by chromatography (15:1, petroleum ether/EtOAc) to obtain the product as a clear oil. R_f 0.27 (15:1, petroleum ether/EtOAc). ^1H NMR (400 MHz, CDCl_3 , δH) 7.35-7.29 (m, 5 H), 6.91-6.80 (m, 3H), 4.52 (s, 2H), 4.46 (s, 2H), 3.89 (s, 3H). ^{13}C NMR (100 MHz, CDCl_3 , δC) 147.7, 146.1, 138.1, 129.9, 128.7, 128.2, 127.8, 12.5, 115.2, 111.8, 72.5, 71.9, 56.0. ESI (m/z) $\text{C}_{15}\text{H}_{17}\text{O}_3^+$: calc. 245.1178; obs. 245.1174

UV-Vis Studies

For typical experiments, the model phosphonate ($p\text{-O}_2\text{NC}_6\text{H}_4\text{OP}(\text{CH}_3)(=\text{O})\text{O}^-\text{Na}^+$), and a chosen QMP were dissolved separately to a concentration of approximately 5.00×10^{-4} M in DMF. The two were added to a test tube (2 mL each) and heated under N_2 for 3 hours at 100°C . The UV-vis absorption was examined directly after heating by adding the reaction mixture (1 mL) to DMF (1 mL). The background hydrolysis of the p -nitrophenol leaving group was monitored at ~ 433 nm in DMF. A second sample of reaction mixture (1 mL) was then added to a pH = 10 solution of NaOH (1 mL) to completely hydrolyze the p -nitrophenol leaving group, which was monitored at 412 nm in a 1:1 DMF/NaOH solution. The measure of the absorbance at 412 nm was an indirect measurement of alkylation of QMP by the model phosphonate. Following the reaction between our precursor and the model phosphonate, addition of base

would cause scission of the P–O(PhNO₂) bond to generate *p*-nitrophenol, which was then monitored appropriately at 412 nm in a 1:1 solution of DMF and pH 10 sodium hydroxide.

A control reaction was performed by adding 2 mL of the model phosphonate (*p*-O₂NC₆H₄OP(CH₃)(=O)O⁻Na⁺) solution to DMF (2 mL), specifically to maintain the same concentration of phosphonate as the alkylation reactions (Figure A.1). The background hydrolysis was monitored at 433nm directly after heating, then measured at 412 nm upon addition of pH = 10 NaOH after heating for 3 h (A = 0.919). This value was then subtracted from the absorbance of the alkylation reactions with **1-4** (Figure A.2), as these solutions were yellow after heating, suggesting a background hydrolysis of *p*-nitrophenoxide that was measured at 433 nm.

However, the background hydrolysis was not included in the percent alkylation calculations for **1-HCl** to **4-HCl** (Figure A.3) because these solutions were clear after heating, suggesting no background hydrolysis of *p*-nitrophenol had occurred during the course of the reaction. The concentration of *p*-nitrophenol was determined by an external standardization method of known concentrations of the chromophore (1.65 x 10⁻⁵ M to 7.00 x 10⁻⁵ M) in a 1:1 DMF:(pH=10) NaOH solution. A linear fit was calculated to fit a Beers Law equation ($y = 18249x + 0.1541$, $R^2 = 0.9934$) to solve for the concentration of the reaction mixtures upon hydrolysis at 412 nm, where y was set equal to the absorbance at 412 nm and x was set equal to the concentration of the known stock solutions of *p*-nitrophenol.

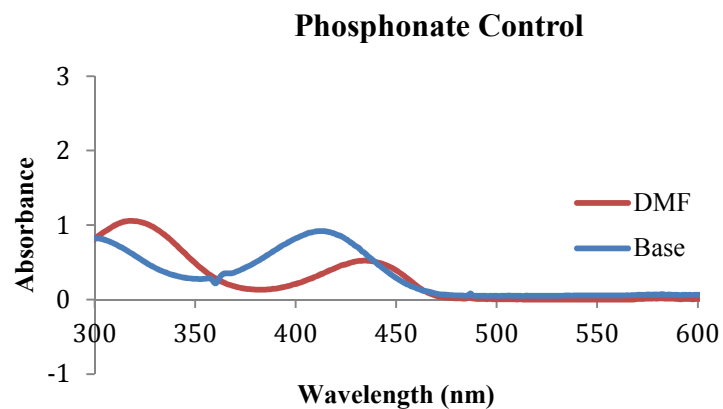


Figure A.1. UV-vis spectrum of control reaction where the model phosphonate (p - $\text{O}_2\text{NC}_6\text{H}_4\text{OP}(\text{CH}_3)(=\text{O})\text{O}^-\text{Na}^+$) was heated in DMF for 3 h at 100°C (red). At this initial reading, p -nitrophenol released in the initial heating was monitored in DMF at 433 nm. After initial measurement, base was added to determine the extent of phosphonate hydrolysis releasing the p -nitrophenoxide group, monitored at 412 nm.

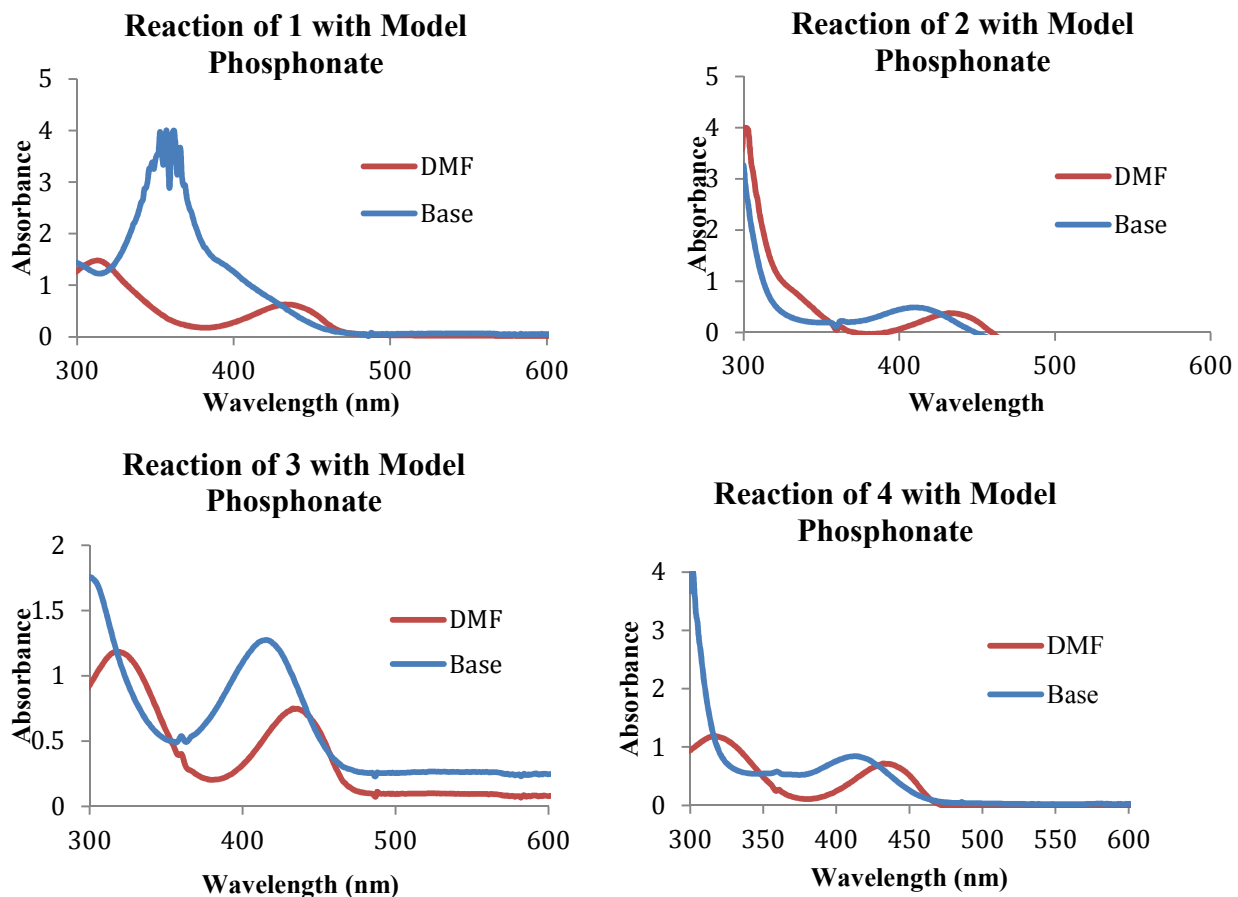


Figure A.2. UV-vis spectrum of **1-4** reacted with model phosphonate ($p\text{-O}_2\text{NC}_6\text{H}_4\text{OP}(\text{CH}_3)(=\text{O})\text{O}^-\text{Na}^+$) at 100°C in DMF. Initial reaction in DMF (red) and after addition of base (blue) showed significant amounts of p -nitrophenol in solution. The signal at 412 nm (blue) did not exceed what was seen in the background reaction, thus no quantifiable alkylation could be observed via this indirect method.

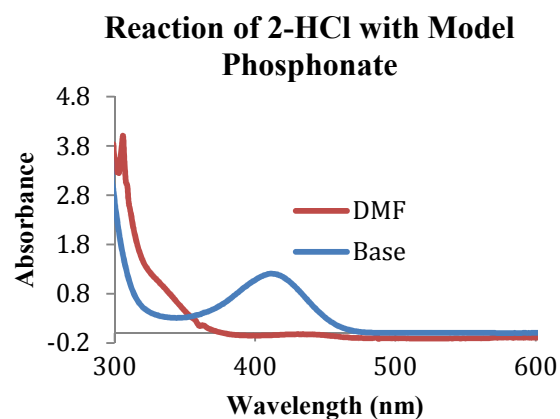
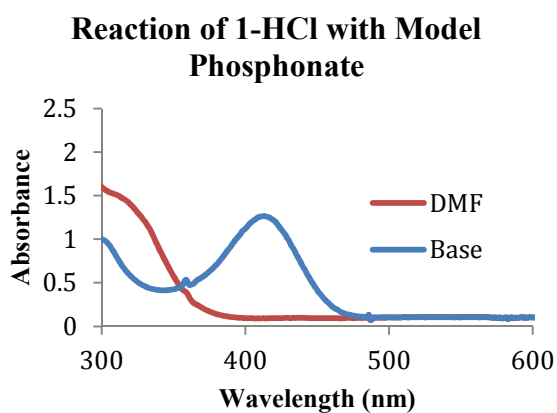
Of the four neutral precursors tested with the model phosphonate, only **3** showed an absorbance at 412 nm (after base-induced hydrolysis of any intermediate alkylated product) above the control reaction. Thus, for **1**, **2**, and **4**, no quantifiable alkylation could be determined. The extent of alkylation for **3** was calculated to be 8.5% based on external standardization methods (Table

A.1), an amount of alkylation similar to the alcohol-based nucleophiles used in our previous experiments.

Table A.1. Percentage alkylation of neutral QMPs using a model phosphonate.

Compound	Absorbance (412 nm)	Percentage Alkylation
1	0.97	N/A ^a
2	0.48	N/A ^a
3	1.26	8
4	0.84	N/A ^a

^a In case of 1–4, background hydrolysis of control reaction was accounted for in the %alkylation calculation. Absorbance at 412 nm of reaction was less than that seen in the control reaction, thus no quantifiable alkylation by QMP could be calculated.



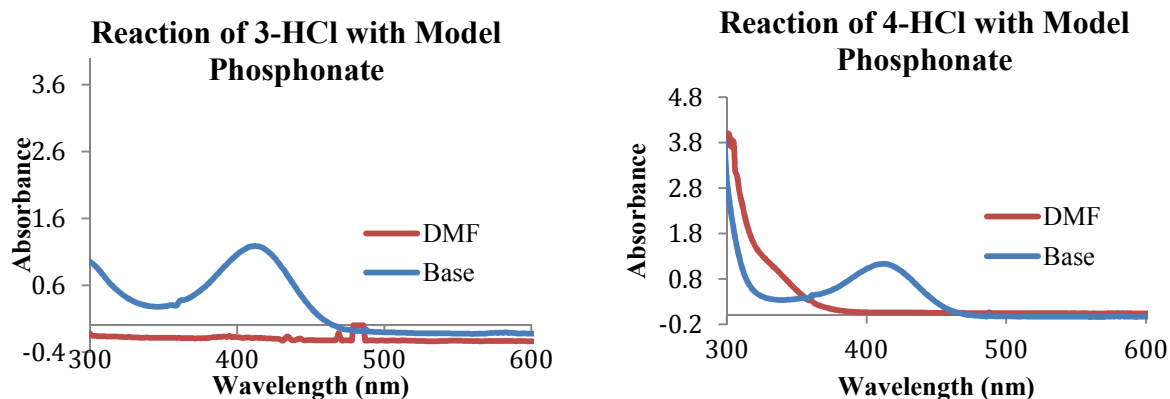


Figure A.3. UV-vis spectra of **1-HCl-4-HCl** reacted with model phosphonate at 100°C in DMF.

Initial reaction of **1-HCl-4-HCl** in DMF (red) showed no evidence of a background reaction (no signal at 433 nm); however, there was a significant signal at 412 nm after addition of base, indicative of base-induced cleavage of *p*-nitrophenol from an intermediate alkylated product. The %alkylation was calculated from an external standardization, ignoring any background hydrolysis.

Presumably, the lack of an observed background reaction in **1-HCl-4-HCl** is due to the presence of the proton on the amine leaving group, although the specific mechanism behind the lack of a background reaction remains unclear. The yellow color assigned to the presence of *p*-nitrophenol only appeared upon addition of base, presumably indicating the cleavage of the chromophore from an intermediate alkylated product. Absorbance at 412 nm in the case of the protonated QMPs showed more substantial alkylation than any of the neutral precursors tested, ranging from 43–50% (Table A.2). However, the UV-vis protocol proved itself to be somewhat unreliable over the course of replicate trials as results were difficult to reproduce over replicate trials. Further, the relatively low amounts of alkylation caused us to think more critically about our indirect method of monitoring alkylation. Namely, we reconsidered the assumption made

about the base-induced hydrolysis of the intermediate alkylated phosphonate and sought other methods to monitor alkylation of a model nucleophile more directly.

Table A Error! No text of specified style in document..2. Percentage alkylation of protonated QMPs using a model phosphonate.

Compound	Absorbance (412 nm)	Percentage Alkylation
1-HCl	1.26	50
2-HCl	1.21	47
3-HCl	1.19	46
4-HCl	1.13	43

HPLC Data

A representative QMP of the neutral (**1**) and protonated (**1-HCl**) form were each reacted with the model phosphonate in water at 100 °C for 3 h and analyzed using the HPLC-MS (ESI-TOF) to identify each of the species in solution after heating. The HPLC analysis was performed on an Agilent G6230A HPLC/TOF mass spectrometer. The components included a CTCPAL auto-injector with 1 µL sample loop, Bin Pump (G42220A) operating at a maximum pressure of 1200 bar, and a solvent ratio of 50:50 water:acetonitrile with 0.1% formic acid for ionization that was flowing at 0.3 mL/min for 3 minutes. The HPLC column was a C-18 50 mm high pressure column without guard. The time-of-flight (TOF) was calibrated daily and data were acquired in positive ion mode with total ion counting turned on. The source parameters for the TOF were: gas temperature of 325 °C, gas flow of 10 L/min, nebulizer of 20 psi, sheath gas temperature of 400 °C and a sheath gas flow of 10 L/min. The scan source parameters were run with a voltage

capacity of 3000. Reference masses during the scan were obtained at 121.0508 and 922.0979 amu.

For each species, only trace amounts of the alkylated product (**b** in Scheme 5) were observed. The major peaks observed in each reaction were **a**, **c**, **e** and **f**. The alkylation products could not be quantified, due to the inability to separate each peak in the HPLC. In the case of **1** (Table A.3) and **1-HCl** (Table A.4), the observed products were identical, due to the identical QMP scaffold for each precursor.

Table A.3. Results from HPLC/ESI-MS-TOF analysis of reaction between **1** and model phosphonate in water at 100 °C for 3 h. Trace amounts of the alkylated product were observed. The major observed products resulted from a dual hydrolysis degradation of the intermediate alkylated product.

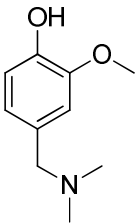
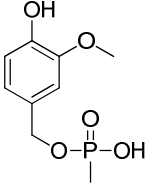
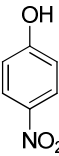
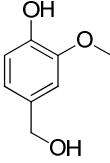
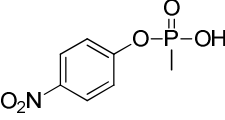
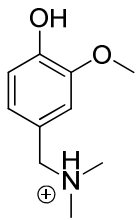
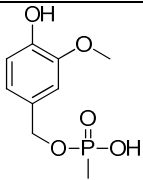
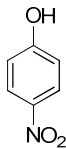
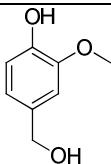
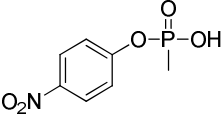
QMP	Hydrolysis Products	Major MS Peaks
	 Exact Mass: 232.0501  Exact Mass: 139.0269	139.0271 232.0496
	 Exact Mass: 154.0630  Exact Mass: 217.0140	154.0621 217.0144

Table A.4. Results from HPLC/ESI-MS-TOF analysis of reaction between **1-HCl** and model phosphonate in water at 100 °C for 3 h. Trace amounts of the alkylated product were observed. The major observed products resulted from a dual hydrolysis degradation of the intermediate alkylated product.

QMP	Hydrolysis Products	Major MS Peaks
	<div style="display: flex; justify-content: space-around; align-items: center;"> <div style="text-align: center;">  <p>Exact Mass: 232.0501</p> </div> <div style="text-align: center;">  <p>Exact Mass: 139.0269</p> </div> </div>	<p>139.0261</p> <p>232.0510</p>
	<div style="display: flex; justify-content: space-around; align-items: center;"> <div style="text-align: center;">  <p>Exact Mass: 154.0630</p> </div> <div style="text-align: center;">  <p>Exact Mass: 217.0140</p> </div> </div>	<p>154.0611</p> <p>217.0136</p>

Computational Methods:

Each of the eight proposed ligands was built with GaussView 4.1.2.¹ Then all eight compounds were optimized with Gaussian 09² using the B3LYP/6-311+G** level of theory using the Polarizable Continuum Model of solvation with water. Several conformations of each ligand were manually generated and optimized in order to attempt to locate each ligand's global energy minimum. Of the optimized structures generated, the lowest energy conformation for each ligand was selected and vibrational frequency analyses were performed at B3LYP/6-311+G** to confirm the geometry was a minimum on the potential energy surface. Then Merz-

Kollman charge calculations were performed on these lowest energy conformations to prepare the ligands for docking simulations.

The receptor structure for AChE was taken from the available crystal structure for human AChE (PDB id 1B41³). Waters, cofactors, and the associated fasciculin-II peptide were then removed from the crystal structure using UCSF Chimera.⁴ Any residues that were missing from the structure after those modifications were then added in based on homology to electric eel AChE (PDB id 1C2B⁵). The aged organophosphorus agent was then placed on Serine 203 to age the active site based on available structures of the aged torpedo enzyme (PDB id 2WG1⁶). Protonation states of the titratable residues were determined using the program pdb2pqr with propKa at neutral pH.⁷ Any missing side chain atoms were replaced in the xLEaP module of AMBER10, from which a mol2 file was obtained with *ff03* charges.⁸ Thirteen representative snapshots were chosen from a five nanosecond molecular dynamics simulation where a sample QMP was placed in the aged AChE active site to be used as receptors in the molecular docking simulations in order to simulate the induced fit of these class of ligands.

Docking simulations of all 8 ligands in each of the 13 receptor frames were carried out in Autodock 4.0.⁹ For each receptor frame, the residues F338, Y341, and W86 of AChE were treated as flexible during the docking simulations in order to minimize some of the steric constraints around the catalytic site due to the protein environment. A 50 x 50 x 50 (Å³) grid box with a grid spacing of 0.275 Å was created and centered on the oxyanion hole. A 2 ns simulation time with explicit TIP3P water solvation was utilized for each docking simulation, and snapshots were taken every 100 fs in order to sample conformations of the equilibrated ligands, resulting in 200 snapshot “poses” per docking simulation. Temperature, density, and KE/PE properties were stable, in addition to stabilization of the backbone RMSD of the AChE structure and binding

orientation during the production MD simulation were used as a metric to confirm equilibration. A total of 13 docking simulations were completed for each ligand, one in each aged receptor frame. In total, this resulted in the production of 2600 snapshot “poses” per ligand. Three representative poses of compound **1** are shown in Figure A.4. Ligands were allowed to sample all torsional motions, while AChE bond lengths and angles were held fixed during the simulation except for the three previously-noted residues that were treated as flexible.

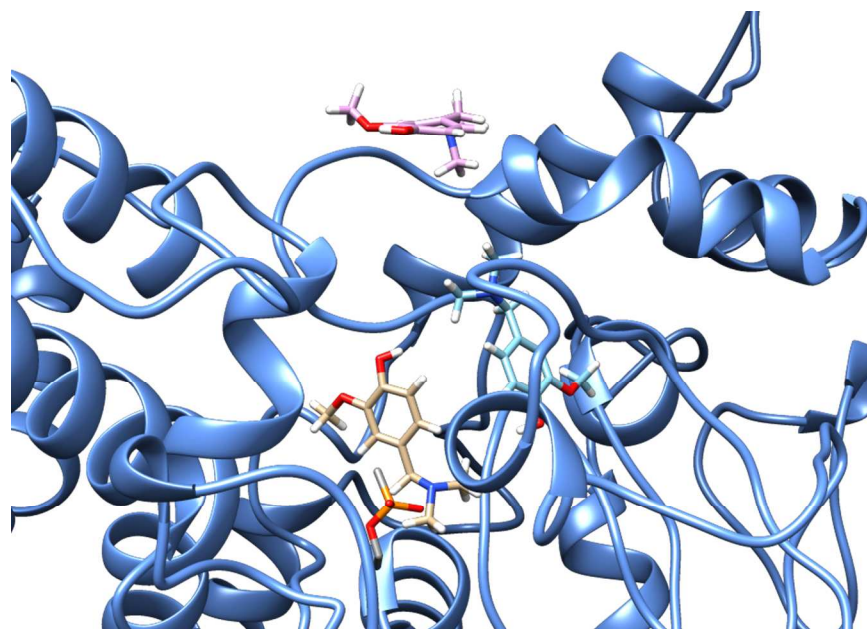


Figure A.4. Three representative different docked poses of **1** interacting with Frame 0200.

Initially, our focus in examining the poses generated from molecular docking was the distance between the phosphorylated serine residue and the benzylic carbon of our QMPs. The reasoning is straightforward as these two atoms would ideally participate in the new bond being formed between the aged AChE (nucleophile) and our QMPs (electrophile). Thus, at first we considered any pose that placed the benzylic carbon of our QMP within 4 Å of the phosphorylated serine residue (**Table A.6**). However, these static snapshots did not produce much evidence to differentiate the neutral and protonated compounds, thus we proceeded on to a molecular dynamics simulation.

Table A.5. Percentage of Molecular Docking Simulation Based on Zoning Criteria.

Compound Name	Percentage of Poses Within 4.0 Å of Aged Serine Residue
1-HCl	37.08
2-HCl	47.19
3-HCl	36.42
4-HCl	27.31
1	35.51
2	46.50
3	36.08
4	24.35

Using the previously proposed eight ligands, the three lowest energy molecular docking snapshots for each of the 13 prepared aged AChE receptor frames as input geometry, molecular dynamics calculations were performed using Sander in AMBER11.¹⁰ The ff03 force field parameters were applied to all residues except for the alkylated Serine 203 residue, which required parameters to be manually calculated due to being non-standard. Explicit hydrogen atoms were added to each ligand manually using UCSF Chimera 1.10¹¹. The tleap module of AMBER11¹ was used to neutralize each system with Na⁺ counter ions, add one of the ligands to the active site, and solvate the protein. The system underwent two minimizations. The first minimization involved 500 steps of steepest decent minimization to push the system away from any local maxima. This was followed by 500 steps of conjugate gradient minimization to converge the system towards the minima. The system was treated with an explicit TIP3P¹² water

solvation model as well as a non-bonded cutoff of 10 angstroms. For the second minimization, the system underwent 1000 steps of steepest decent minimization followed by 1500 steps of conjugate gradient minimization. This system was also treated with an explicit TIP3P water solvation model as well as a non-bonded cutoff of 10 angstroms. After the minimizations, the system was heated linearly from 0 K to 300K over 20 ns (10000 steps of 2 ps). The pressure was set at 1 atm without pressure control, and the seed for the random number generator was set to -1 (random at each start) to eliminate any pseudorandom repeats biasing the Langevin thermostat¹³. After this equilibration, MD was performed on the solvated system over 1 ns (500,000 steps of 2 ps) with the temperature and pressure held constant at 300K and 1 atm.

An empirical study of our MD results, combined with knowledge of the AChE active site, bottleneck, and gorge mouth, allowed us to examine the positioning of our ligands within the enzyme. To better communicate the relative position of our ligands throughout the enzyme, zoning criteria were established to describe the various regions of AChE. These regions were created by measuring the distance from the phosphorylated serine residue of aged AChE (described above) to the benzylic carbon of our QMP, which would be the target electrophile. Our zones for the residence of the QMPs during our MD simulation were then established as: Active Site (0-5 Å), a zone from 7-9.5 Å that largely incorporated the Bottleneck region, and a zone from 10-15 Å encompassing the Gorge Mouth, all as closed bounds. The results below (**Table A.7**) include regions between these zones and “Other”, which would be greater than 15 Å. Unquestionably, the protonated compounds perform better at accessing the active site than the neutral compounds, which spend the majority of the time outside the active site.

Atom coordinates and parameters of molecular models can be accessed in a separate appendix file (appendix coordinates and parameters.docx).

Table A.7. Percentage of Molecular Dynamics Simulation Based on Zoning Criteria.

Compound Name	% Active Site (0-5Å°)	7-9.5Å (% Bottleneck)	10-15Å (% Gorge Mouth)
1-HCl	44.84	3.70	23.86
2-HCl	50.46	7.25	14.06
3-HCl	44.56	10.71	22.52
4-HCl	37.39	9.92	25.83
1	11.84	28.45	13.94
2	24.14	35.60	6.66
3	6.02	25.44	16.76
4	8.92	34.16	28.56

Determination of Inhibition Characteristics of QMPs against Native AChE¹⁴

Electric eel AChE, acetylthiocholine (ATC) and 5,5'-dithiobis-(2-nitrobenzoic acid) (DTNB) were all purchased from Sigma-Aldrich. Reaction solutions containing DTNB (1 mM), ATC (0~4 mM), QMP (0~1.5 mM) and AChE (25 ng/mL) were prepared in 50 mM phosphate buffer (pH = 7.0). Absorbance at 412 nm was measured over 7 min at room temperature (21~26 °C) to monitor the rate of ATC hydrolysis. Each sample was tested in 4~6 replicate wells on a clear 96-well microplate. Acquired data were nonlinearly fitted into following equation of mix-type inhibition:

$$r = \frac{V_{\max}[S]}{[S] \left(1 + \frac{[I]}{\alpha K_i}\right) + K_m \left(1 + \frac{[I]}{K_i}\right)}$$

where r stands for the rate of substrate (ATC) consumption, V_{\max} for the maximum rate, $[S]$ for the concentration of substrate, $[I]$ for the concentration of inhibitor (QMP in this case), K_i for the inhibition constant and K_m for the Michaelis constant, using the software GraphPad Prism 6

(Figure A.5.). Constant α reveals the type of inhibition. When $\alpha = 1$, the inhibition is considered as noncompetitive. The greater α , the more competitive the inhibitor is.

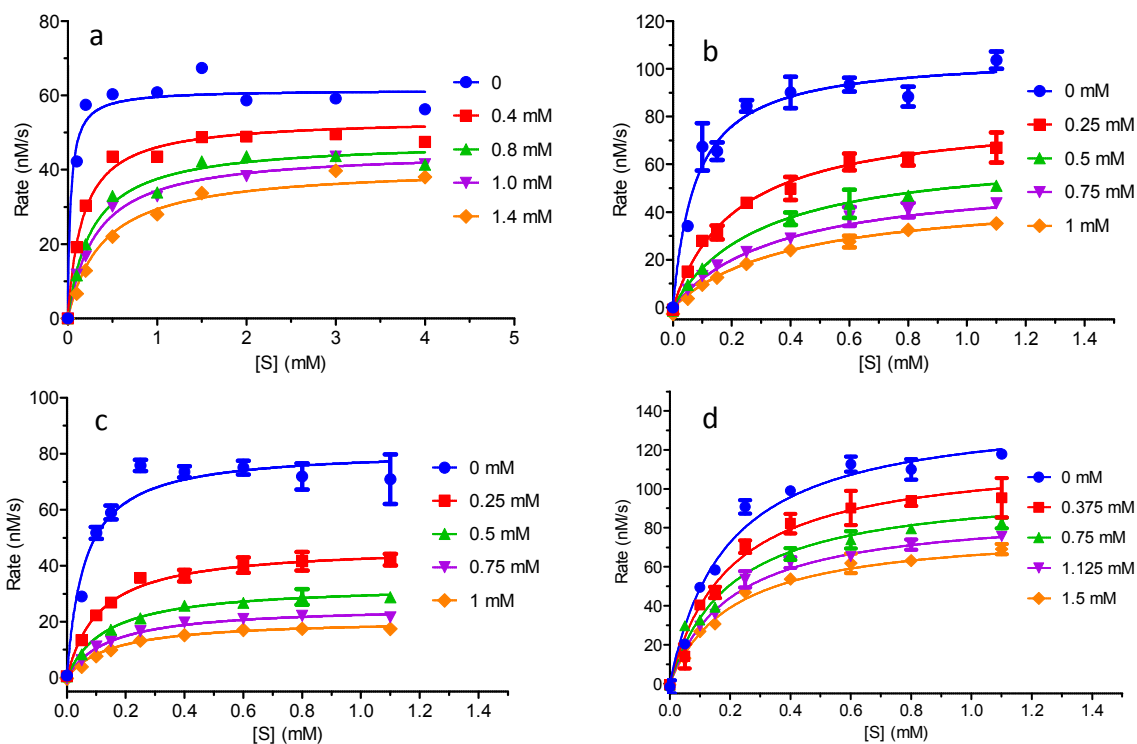


Figure A.5. Rate of ATC hydrolysis indicating AChE activity in the presence of **1-HCl** (a), **2-HCl** (b), **3-HCl** (c) and **4-HCl** (d) at various concentrations of QMPs and ATC.

Procedures for Aging of AChE

Caution: This experiment involves the use of a toxic OP compound. Please use it in a well ventilated fume hood and wear personal protection equipment. Contaminated glassware and consumables should be treated with concentration NaOH or KOH solution for decontamination.

50 μL of electric eel AChE (~ 30 units in 40 mM phosphate buffer, pH 7.0, containing 100 μg bovine serum albumin for stabilization and 0.02% NaN_3 as preservative) was reacted with a soman analogue (**5**, 0.2 mM \times 5 μL in 2% acetonitrile, mixture of all four stereo isomers; structure shown in Figure A.6) for 2 h at 37 $^\circ\text{C}$, then diluted to 100 μL with the buffer. All reagents were removed by Sephadex G-25 spin columns (equilibrated with pH 8.0 phosphate). 4 μL \times 100 mM 2-PAM was added to reactivate residual inhibited AChE (unaged), which might be the product of the stereo isomer or isomers of slower aging. It was also removed from the solution after 2 d of reaction at 37 $^\circ\text{C}$. The enzyme was treated again with **5** (1 μL) for 1 h at pH 7.0, which was removed with Sephadex at pH 8.0. 1 μL \times 2% NaN_3 was added after the spin. A positive control of native AChE was prepared in parallel using blank solvents instead of **5** solution.

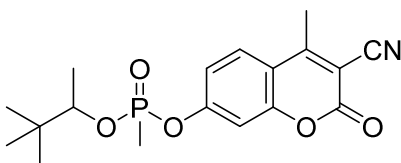


Figure A.6. Soman analogue (**5**) used to prepare methylphosphonate-aged AChE

Procedures for Realkylation and Reactivation of Aged AChE

1.8 μL of aged electric eel AChE solution was mixed with bovine serum albumin solution (90 μL \times 1 g/L), QMP solution (4 μL \times 100 mM) and NH_4F solution (4 μL \times 100 mM). All reagent solutions were prepared in 40 mM phosphate buffer (pH 8.0). The negative and the

positive controls were prepared in parallel with aged and native AChE, respectively, with the QMP solution replaced by blank buffer. The 2-PAM control was prepared by replacing the QMP solution with 4 mM 2-PAM. The mixed solutions were reacted at 37 °C for 24 h. 4 μ L \times 100 mM 2-PAM was then added for reactivation. All reagents were removed 1 h later by a size exclusion spin plate (Zeba, purchased from Thermo Scientific).

AChE activity was determined by Ellman's assay. 20 μ L of each sample was added to a clear microplate well filled with 180 μ L of assay solution containing 0.56 mM ATC and 1.1 mM DTNB. Each sample was analyzed in 4 replicate wells. Absorption at 412 nm was monitored for 10 min. The AChE activity was calculated based on the initial rate of this pseudo zeroth-order reaction.

References

¹GaussView, Version 4.1.2, Dennington, Roy; Keith, Todd; Millam, John. Semichem Inc., Shawnee Mission, KS, **2009**.

²Gaussian 09, Revision D.01, Frisch, M. J.; Trucks, G. W.; Schlegel, H. B.; Scuseria, G. E.; Robb, M. A.; Cheeseman, J. R.; Scalmani, G.; Barone, V.; Mennucci, B.; Petersson, G. A.; Nakatsuji, H.; Caricato, M.; Li, X.; Hratchian, H. P.; Izmaylov, A. F.; Bloino, J.; Zheng, G.; Sonnenberg, J. L.; Hada, M.; Ehara, M.; Toyota, K.; Fukuda, R.; Hasegawa, J.; Ishida, M.; Nakajima, T.; Honda, Y.; Kitao, O.; Nakai, H.; Vreven, T.; Montgomery, J. A., Jr.; Peralta, J. E.; Ogliaro, F.; Bearpark, M.; Heyd, J. J.; Brothers, E.; Kudin, K. N.; Staroverov, V. N.; Kobayashi, R.; Normand, J.; Raghavachari, K.; Rendell, A.; Burant, J. C.; Iyengar, S. S.; Tomasi, J.; Cossi, M.; Rega, N.; Millam, N. J.; Klene, M.; Knox, J. E.; Cross, J. B.; Bakken, V.; Adamo, C.; Jaramillo, J.; Gomperts, R.; Stratmann, R. E.; Yazyev, O.; Austin, A. J.; Cammi, R.; Pomelli, C.; Ochterski, J. W.; Martin, R. L.; Morokuma, K.; Zakrzewski, V. G.; Voth, G. A.; Salvador, P.; Dannenberg, J. J.; Dapprich, S.; Daniels, A. D.; Farkas, Ö.; Foresman, J. B.; Ortiz, J. V.; Cioslowski, J.; Fox, D. J. Gaussian, Inc., Wallingford CT, **2009**.

³Kryger, G.; Harel, M.; Giles, K.; Toker, L.; Velan, B.; Lazar, A.; Kronman, C.; Barak, D.; Ariel, N.; Shafferman, A.; Silman, I.; Sussman, J. L. *Acta Crystallogr., Sect. D* **2000**, *56*, 1385-1394.

⁴Petterson, E. F.; Goddard, T. D.; Huang, C. C.; Couch, G. S.; Greenblatt, D. M.; Meng, E. C.; Ferrin, T. E. *J. Comput. Chem.* **2004**, *25*, 1605-1612.

⁵Bourne, Y.; Grassi, J.; Bougis, P. E.; Marchot, J. *J. Biol. Chem.* **1999**, *274*, 30370-30376.

-
- ⁶ Sanson, B.; Nachon, F.; Colletier, J. P.; Froment, M. T.; Toker, L.; Greenblatt, H. M.; Sussman, J. L.; Ashani, Y.; Masson, P.; Silman, I.; Weik, M. *J. Med. Chem.* **2009**, *52*, 7593-7603.
- ⁷ a) Dolinski, T. J.; Nielsen, J. E.; McCammon, J. A.; Baker, N. A. *Nuc. Acids Res.* 2004, *32*, W665-W667. b) Olsson, M. H. M.; Søndergard, C. R.; Rostkowski, M.; Jensen, J. H. *J. Chem. Theory Comput.* **2011**, *7*, 525-537.
- ⁸ Case, D. A.; Darden, T. A.; Cheatham, T. E., III; Simmerling, C. L.; Wang, J.; Duke, R. E.; Luo, R.; Crowley, M.; Walker, R. C.; Zhang, W.; Merz, K. M.; Wang, B.; Hayik, S.; Roitberg, A.; Seabra, G.; Kolossváry, I.; Wong, K. F.; Paesani, F.; Vanicek, J.; Wu, X.; Brozell, S. R.; Steinbrecher, T.; Gohlke, H.; Yang, L.; Tan, C.; Mongan, J.; Hornak, V.; Cui, G.; Mathews, D. H.; Seetin, M.G.; Sagui, C.; Babin, V.; Kollman, P. A. AMBER 10, University of California, San Francisco, **2008**.
- ⁹ Morris, G. M.; Goodsell, D. S.; Halliday, R. S.; Huey, R.; Hart, W. E.; Belew, R. K.; Olson, A. J. *J. Comput. Chem.* **1998**, *19*, 1639-1662.
- ¹⁰ Case, D. A.; Darden, T. A.; Cheatham, T. E., III; Simmerling, C. L.; Wang, J.; Duke, R. E.; Luo, R.; Crowley, M.; Walker, R. C.; Zhang, W.; Merz, K. M.; Wang, B.; Hayik, S.; Roitberg, A.; Seabra, G.; Kolossváry, I.; Wong, K. F.; Paesani, F.; Vanicek, J.; Wu, X.; Brozell, S. R.; Steinbrecher, T.; Gohlke, H.; Yang, L.; Tan, C.; Mongan, J.; Hornak, V.; Cui, G.; Mathews, D. H.; Seetin, M.G.; Sagui, C.; Babin, V.; Kollman, P. A. AMBER 10, University of California, San Francisco, 2008.
- ¹¹ Pettersen, E. F.; Goddard, T. D.; Huang, C. C.; Couch, G. S.; Greenblatt, D. M.; Meng, E. C.; Ferrin, T. E. *J. Comput. Chem.* **2004**, *25*, 1605-1612.
- ¹² Jorgensen, W. L.; Chandrasekhar, J.; Madura, J. D.; Impey, R. W.; Klein, M. L. Comparison of simple potential functions for simulating liquid water. *J. Chem. Phys.* **1983**, *79*, 926-935.
- ¹³ Cerutti DS, Duke, B., *et al.*, "A Vulnerability in Popular Molecular Dynamics Packages Concerning Langevin and Andersen Dynamics", *J. Chem. Theory Comput.* **2008**, *4*, 1669-1680.
- ¹⁴ Ellman, G.L. Tissue Sulfhydryl Groups. *Arch. Biochem. Biophys.* **1959**, *82*, 70-77.